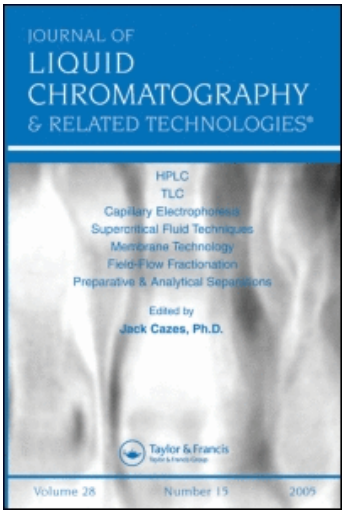

Journal of Liquid Chromatography & Related Technologies
Publication details, including instructions for authors and subscription information:
http://www.informaworld.com/smpp/title~content=t713597273

Design of Experiments for Capillary Electrophoretic Enantioresolution of Tamsulosin using Sulfated-β-Cyclodextrin as Chiral Selector

Yu Ping Zhang[a]; Yi Jun Zhang[a]; Wen Jun Gong[a]; Shu Ming Wang[b]; Hui Yong Xue[b]; Kwang Pill Lee[c]
[a] Henan Institute of Science and Technology, Xinxiang, P. R. China [b] Beijing Kangbeide Pharmaceutical Development Company Limited, Beijing, P. R. China [c] Department of Chemistry, Graduate School, Kyungpook National University, South Korea

To cite this Article Zhang, Yu Ping , Zhang, Yi Jun , Gong, Wen Jun , Wang, Shu Ming , Xue, Hui Yong and Lee, Kwang Pill(2007) 'Design of Experiments for Capillary Electrophoretic Enantioresolution of Tamsulosin using Sulfated-β-Cyclodextrin as Chiral Selector', Journal of Liquid Chromatography & Related Technologies, 30: 2, 215 — 234
To link to this Article: DOI: 10.1080/10826070601064375
URL: http://dx.doi.org/10.1080/10826070601064375

Journal of Liquid Chromatography & Related Technologies®, 30: 215–234, 2007

ISSN 1082-6076 print/1520-572X online
DOI: 10.1080/10826070601064375

Design of Experiments for Capillary Electrophoretic Enantioresolution of Tamsulosin using Sulfated-β-Cyclodextrin as Chiral Selector

Yu Ping Zhang, Yi Jun Zhang, and Wen Jun Gong
Henan Institute of Science and Technology, Xinxiang, P. R. China

Shu Ming Wang and Hui Yong Xue
Beijing Kangbeide Pharmaceutical Development Company Limited, Beijing, P. R. China

Kwang Pill Lee
Department of Chemistry, Graduate School, Kyungpook National University, South Korea

Abstract: A method of quickly determining tamsulosin enantiomers by capillary zone electrophoresis with a photodiode array detector was developed. Response surface methodologies based on three-level, three-variable designs such as Box-Behnken design, central composite face-centered, and central composite circumscribed design, were comparatively used for the optimization with respect to selector concentration, applied voltage, and column temperature. Statistical interpretation of the variables on different responses, such as resolution and migration time of the last isomer were performed. The optimum conditions of these variables were predicted by using a second-order polynomial model, fitted to the results obtained by applying three designs. The response surface plots using three experimental designs revealed a separation optimum with 100 mM tris (hydroxymethyl) aminomethane buffered with phosphoric acid to pH = 2.5, concentration of sulfated-β-cyclodextrin, 0.15% (W/V), column temperature 25°C, and applied voltage of 25 kV. The significance of the statistical designs was confirmed by the generally good agreement obtained between predicted responses and actual experimental data. We have concluded that

Address correspondence to Prof. Yu Ping Zhang, Henan Institute of Science and Technology, Xinxiang 453003, P. R. China. E-mail: beijing2008zyp@163.com or yupzhang@hotmail.com

experimental designs offer a rapid means of optimizing several variables, and provide an efficient test for the robustness of the analytical method.

Keywords: Tamsulosin, Response surface methodology, Capillary electrophoresis, Chiral separation, Sulfated-β, -cyclodextrin, Experimental design

INTRODUCTION

Many methods have been developed in order to optimize the parameters of interest in capillary electrophoresis and related techniques.[1,2] In chemometric approaches, experimental measurements are performed in such a way that all variables vary together. An objective function is utilized in which the analyst introduces the desired criteria (selectivity, resolution, time of analysis). The advantage of chemometrics tools is that no explicit models are required, and when models are available optimization is easier to perform by regression methods. Optimization of a CE separation condition is a critical step, since the wide array of variables such as applied voltage, buffer composition, ionic strength, temperature, capillary length, and injection time can influence the separation efficiency, migration time, resolution, etc., and a complete and quite general physicochemical model in CE is still missing.[3–5] One approach to achieve an optimal separation is to vary the experimental parameter steps while keeping other parameters constant. But, the search for the optimal separation condition by this approach requires too much experimental work, and is tedious and time consuming. Furthermore, when interaction appears, an independent univariate optimization is not appropriate to find the best experimental conditions, since the influence of any given variable depends on the magnitude of another variable.

A suitable alternative to overcome the aforementioned shortcomings lies in experimental design techniques. Moreover, the number of experiments to be carried out can be reduced drastically when following these chemometric strategies.[6–9] Chemometrics are involved in the preliminary stages for the establishment of a CE method and the analysis of CE data to extract the maximum amount of significant information. It allows a large number of parameters to be screened simultaneously, and to achieve this in a small number of mathematical runs is the most important aspect of mathematical design and will provide a mathematical framework. Experimental designs such as Plackeet-Burman design (PBD), Box-Behnken design (BBD), central composite face-centered design (CCF), central composite circumscribed design (CCC), full-factorial design (FFD), etc., have been used for CE separation studies.[10–16] Several studies have been reported on the use of multivariate statistical analysis to optimize CE methods. Depending on the design, the response model can show the relationship between each parameter. BBD, CCF, and CCC are the response surface methods used to optimize CE separation.[17,18] As an efficient statistical tool for optimization

of multiple variables, it can be performed respectively to predict the best performance conditions by using a minimum number of experiments.

With a growing demand to explore the different toxicities and metabolic pathways of drug enantiomers, pharmaceutical companies are putting increasing efforts into the characterization of optically active drugs, with respect to their optical purity. (±) 5-[2 (R, S)-{[2-(*o*-ethoxyphenoxy) ethyl]amino} propyl]-2-methoxy-benezensulfonamide (tamsulosin) hydrochloride exists in two enantiomeric forms but only R-isomer is the pharmaceutically active component. Fast quantification of the tamsulosin enantiomers is very important for quality control of the synthesis procedure, as well as for pharmacological and pharmacokinetic studies. Several methods have been used for determining tamsulosin in different matrices, including high performance liquid chromatography (HPLC),[19,20] liquid chromatography with atmospheric pressure chemical ionization tandem mass spectrometry (LC-MS-MS),[21] liquid chromatography with electrospray ionization-mass spectrometry (LC-ESI-MS).[22] Capillary zone electrophoresis (CZE) possesses the advantages of short analysis time, small consuming sample, high separation efficiency, simple experimental operation, and so on. A recent paper revealed that the baseline separation of tamsulosin enantiomers could be obtained within 12 min using sulfated-β-cyclodextrin (S-β-CD) as the chiral selector. The typical electropherogram of the studied enantiomers was obtained under the optimized conditions (pH 2.5; phosphate/Tris buffer concentration 100 mM; concentration of S-β-CD 1.7 mM; temperature 18°C; applied voltage +20 kV with a polyacrylamide-coated capillary.[23]

In the present work, BB, CCF, and CCC designs have been comparably performed to determine the optimal separation conditions by CZE. Increased chiral resolution and migration time can be obtained using the experimental design methodology, instead of the above method using the coated capillaries. Furthermore, in order to find the best compromise between several responses, a multi criteria decision making approach was used, in which the resolution response and migration time response can be simultaneously optimized. Baseline separation of the enantiomers has been obtained quickly during 3 min, with a resolution greater than 1.5.

EXPERIMENTAL

Chemicals

R,*S*-Tamsulosin hydrochloride (TH) standards and the tamsulosin hydrochloride product were provided by Beijing Kangbeide Pharmaceutical Development Company, China, sulfated-β-cyclodextrin sodium salt (typical substitution 7–11 mol/mol) was purchased from Beijing Bailingwei Chemical Reagent Company, HCl, tris (hydroxymethyl) aminomethane were purchased from Beijing Chemical Reagent Company, double-distilled

water was obtained from a super-purification system (Danyangmen Corporation, Jiangshou, China). The racemic test mixtures of both enantiomers were used freshly prepared to prevent degradation. Standard stock solutions with a concentration of 1000 μg/mL were prepared in deionized water, with further dilution before the operation. All electrolyte solutions and samples were filtered through 0.45 μm pore size filters and degassed in an ultrasonic bath for 15 min before use.

Apparatus

CE separation was performed with a HP^{3D} CE system with a photodiode array detector, an autosampler, and a power supply able to deliver up to 30 kV (Agilent Technologies, Inc., Walbronn, Germany). A CE ChemStation (Hewlett-Packard) software was used for instrument control, data acquisition, and data handling. All experiments were carried out in the cationic mode (anode at the inlet and cathode at the outlet). An uncoated fused silica capillary of 50 μm I.D. and 33 cm (24.5 cm effective length) was employed throughout all experiments. The capillary was conditioned before each analysis by flushing successively with H_2O, and buffer for 5 min, respectively. Samples were injected with pressure at 50 mbar for 5 s and separated at the operating voltage.

RESULTS AND DISCUSSION

Statistical Experimental Design

The pH of the carrier electrolyte has a dramatic influence on the separation of the tamsulosin enantiomers. Tamsulosin has a pK value about 8.74 and is positively charged at acidic and neutral pH values. The baseline resolution was obtained in the pH range 3.0–3.5, worse resolution and faster migration times were observed at higher pH.[23,24] This electrophoretic behavior of the analyte is probably related to the change of the EOF. EOF at pH $>$ 3.5 became considerable; therefore, short migration times were obtained. Accordingly, there was not enough time allowed for interactions between the selector and the analyte. Also, the enantioseparation mechanism involved included the formation of inclusion complexes, which could be unstable at pH greater than 3.5. At lower pH (about 2.5) the intermolecular interactions, especially the hydrogen bonding, became more available between the polar functional groups of the CD and the analyte. Secondly, at lower pH the basic amino group of the analyte would be protonated (positively charged), thus, the inclusion CD-analyte complex formed would have a better electrophoretic migration within the applied electric field and would enhance effective separation. Note, that the presence of the sulfate substituents on the CDs allows

ion-exchange or electrostatic interactions in addition to more traditional inclusion complexation usually invoked when considering stereospecific interactions with CDs. These interactions contribute to the improvement of the enantioseparation of the analyte under study. In our study, it was kept constant at pH 2.5.

The resolution of the tamsulosin enantiomers increased with increasing concentration of S-β-CD in the buffer. S-β-CD migrates in the opposite direction to the R,S-tamsulosin and to the migration of the electroosmotic flow (countercurrent mode). The good separation ability of S-β-CD was ascribed to enhanced hydrogen bonding of the analyte with the sulfonic acid group of the chiral selector, possible ion-pair interactions, and use of the countercurrent separation mode. The migration order of the enantiomers was R-tamsulosin before S-tamsulosin. The migration order was the same in the whole studied concentration range of S-β-CD. Peak distortion was observed with increasing concentration of the selector according to the relative research.[24] For this reason, the best concentration of S-β-CD of 0.1% (W/V) was chosen as the central point for optimization. Increasing the voltage results in shortening migration time and improving the separation efficiency. However, as voltage is further increased, excessive Joule heating results in band broadening. Hence, maximum resolution is obtained by maintaining the voltage below the level at which Joule heating becomes a limiting factor, so an organic buffer was used in our studies. The separation temperature affects the mobility of the species, and of the EOF, by changing the viscosity of the electrolyte. In our study, the above two variables was chosen for the optimization.

Initial method screening to determine the most significant variables for the analytes did not require an experimental design approach due to the previous CE studies.[23,24] As shown in Table 1, three important variables were chosen for the optimization designs, namely the concentration of selector, applied voltage, and temperature. In order to calculate quadratic regression model coefficients, each design variable has to be studied at three distinct levels or at least five levels.

BB and CCF and CCC models were comparatively used for the multivariable approach. For the BB design, the experimental plan for a three-parameter

Table 1. Coded and true values of variables of the BB, CCF and CCC design models

	Code		Level				
Variables	Coded value	True value	−1.682	−1	0	1	1.682
Concentration (mM)	X_1	x_1	0.016	0.05	0.10	0.15	0.18
Voltage (kV)	X_2	x_2	11.59	15	20	25	28.41
Temperature (°C)	X_3	x_3	11.59	15	20	25	28.41

design is laid out according to the following pattern: two variables have a combination of their extreme levels, while the other is set to its mean value. For a three-parameter design, all experimental points are located on the edges of a cube around the centre points (Figure 1a). The CCF and CCC designs are based on a full factorial design, which is augmented by centre points, axial or start points (Figure 1b and 1c). There are, therefore, 8 cube points (for a full factorial) with levels of -1 and $+1$, 6 axial or start points with levels of $-\alpha$ and $+\alpha$, and 6 replicates of the centre point. Depending on the α value, three types of models are distinguished: central composite face centre if $\alpha = 1$, central composite circumscribed if $\alpha > 1$, and central composite inscribed (CCI) if $\alpha < 1$. The first type is spherical designs, while the CCF and CCI are cubic designs. Here, for three variables and three or five levels, a total of 20 experiments were considered. As with the CCD model, the BB design is a response surface method, used to examine the relationship between one or more response variables and a set of quantitative experimental parameters. The BBD is not directly based on a full factorial design, as it uses middle points instead of corner points. The BB design requires fewer experiments than CCF and CCC, but covers a slightly smaller experimental region. It is also a spherical design.

The levels of three variables for three designs were shown in Table 1. For the BB and CCF designs, maximum and minimum concentrations for selectors (x_1) were fixed as 0.05% and 0.15%, respectively. Likewise, an operation voltage (x_2) and temperature (x_3) were chosen as $15 \sim 25$ kV and $15 \sim 25^{\circ}$C, respectively. For the CCC design, five levels of three variables should be performed with a α value of 1.682. The BB model, with a total of seventeen experiments, the twelve middle points of the edges on a cube and 5 centre points, the CCF and CCC models, with a total of twenty experiments, were depicted in Tables 2–4, respectively. All other experimental

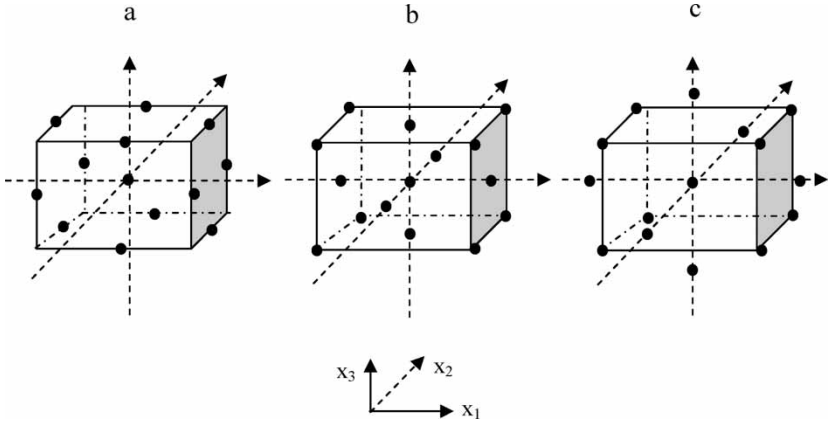

Figure 1. The representation of BB, CCF, and CCC models.

Table 2. Experimental design and response results using BBD model

Run	x_1	x_2	x_3	R_s Exp.	Pred.	t_2 Exp.	Pred.
1	−1	−1	0	0.84	0.80	7.50	7.43
2	1	−1	0	2.65	2.67	8.68	8.65
3	−1	1	0	0.49	0.47	2.72	2.75
4	1	1	0	1.62	1.66	2.93	3.00
5	−1	0	−1	0.86	0.88	4.41	4.48
6	1	0	−1	2.59	2.56	5.56	5.59
7	−1	0	1	0.63	0.66	4.28	4.25
8	1	0	1	2.07	2.05	4.68	4.61
9	0	−1	−1	2.03	2.05	8.49	8.49
10	0	1	−1	1.36	1.35	3.08	2.98
11	0	−1	1	1.64	1.65	7.44	7.54
12	0	1	1	1.03	1.01	2.71	2.71
13	0	0	0	1.64	1.63	4.71	4.65
14	0	0	0	1.63	1.63	4.64	4.65
15	0	0	0	1.64	1.63	4.64	4.65
16	0	0	0	1.62	1.63	4.62	4.65
17	0	0	0	1.62	1.63	4.64	4.65

Table 3. Experimental design and response results using CCF model

Run	x_1	x_2	x_3	R_s Exp.	Pred.	t_2 Exp.	Pred.
1	−1	−1	−1	1.02	0.99	7.39	7.52
2	1	−1	−1	2.85	2.90	10.21	9.96
3	−1	1	−1	0.58	0.61	2.78	2.75
4	1	1	−1	1.78	1.76	3.30	3.33
5	−1	−1	1	0.79	0.80	6.43	6.40
6	1	−1	1	2.45	2.42	8.10	8.12
7	−1	1	1	0.63	0.58	2.41	2.66
8	1	1	1	1.40	1.43	2.65	2.51
9	−1	0	0	0.80	0.84	4.46	4.15
10	1	0	0	2.26	2.22	4.97	5.30
11	0	−1	0	1.85	1.85	7.72	7.86
12	0	1	0	1.17	1.17	2.79	2.67
13	0	0	−1	1.80	1.77	5.03	5.16
14	0	0	1	1.48	1.51	4.29	4.19
15	0	0	0	1.64	1.63	4.71	4.63
16	0	0	0	1.63	1.63	4.64	4.63
17	0	0	0	1.64	1.63	4.64	4.63
18	0	0	0	1.62	1.63	4.62	4.63
19	0	0	0	1.62	1.63	4.64	4.63
20	0	0	0	1.61	1.63	4.58	4.63

Table 4. Experimental design and response results using CCC model

Run	x_1	x_2	x_3	R_s Exp.	Pred.	t_2 Exp.	Pred.
1	−1	−1	−1	1.02	0.88	7.39	7.55
2	1	−1	−1	2.85	2.92	10.21	10.03
3	−1	1	−1	0.58	0.55	2.78	2.61
4	1	1	−1	1.78	1.83	3.30	3.22
5	−1	−1	1	0.79	0.72	6.43	6.48
6	1	−1	1	2.45	2.46	8.10	8.24
7	−1	1	1	0.63	0.54	2.41	2.57
8	1	1	1	1.4	1.52	2.65	2.46
9	−1.682	0	0	0	0.19	3.76	3.62
10	1.682	0	0	2.88	2.72	5.44	5.61
11	0	−1.682	0	1.71	1.78	11.39	11.28
12	0	1.682	0	0.76	0.72	2.11	2.26
13	0	0	−1.682	1.78	1.80	5.29	5.44
14	0	0	1.682	1.4	1.41	4.00	3.90
15	0	0	0	1.64	1.63	4.71	4.63
16	0	0	0	1.63	1.63	4.64	4.63
17	0	0	0	1.64	1.63	4.64	4.63
18	0	0	0	1.62	1.63	4.62	4.63
19	0	0	0	1.62	1.63	4.64	4.63
20	0	0	0	1.61	1.63	4.58	4.63

plans and runs were randomized to exclude any bias. The resolution response (R_s) and the migration time (t_2) were monitored during processing. The calculated responses for the analytes were also respectively included in Tables 2, 3, and 4.

In order to define the relationship between the responses and the variables, a quadratic regression model should be applied on the basis of a multiple linear regression (MLR). The selected model included 10 coefficients, the constant term, B_0, three main effects, three quadratic terms, and three interaction terms, as indicated in the equation:[25–27]

$$y = B_0 + \sum_{i=1}^{n} B_i x_i + \sum_{i=j=1}^{n} B_{ij} x_i x_j$$

In our studies, it can be changed into the following equation according to the n value and the coded values of three variables as follows:

$$y = B_0 + B_1 X_1 + B_2 X_2 + B_3 X_3 + B_{12} X_1 X_2 + B_{13} X_1 X_3 + B_{23} X_2 X_3 + B_{11} X_1^2 + B_{22} X_2^2 + B_{33} X_3^2$$

Where y is the response to be modeled (R_s and t_2), B_i are the coefficients of the models by MLR, X_1 is selector concentration (in coded variable), X_2 is the

operation voltage (in coded variable), and X_3 is the capillary temperature (in coded variable).

Coefficients used for three mathematical models of different responses could be calculated with the help of Design Expert 7.0 Software, which have been calculated and plotted from Figure 2a and 2b. The comparative effects for three models have been clearly shown. When the coefficient is not included in the 95% confidence interval, this means that it is statistically different from 0 and, therefore, the variable associated to this coefficient has a significant influence on response. If it is positive, it favorably influences response whether it represents a main or quadratic effect or a first-order interaction.

As shown in Figure 2a, all terms except T^2 and V * T, have high significant influences on resolution for BB designs; all terms but T^2 have high significant influences for CCF models; all terms but T^2, C * T, and V * T have

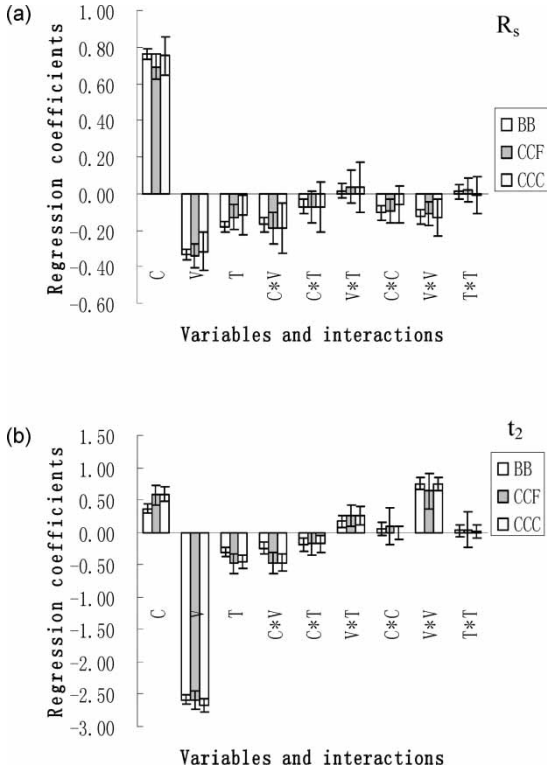

Figure 2. (a) The relationship between the resolution response and the coefficients of three models with corresponding SD; (b) The relationship between migration time of the second peak and the coefficients of three models with corresponding SD. Error bars represent $\pm$SD at level 0.05.

high significant influences for CCC models. As for retention time in Figure 2b, all terms except C^2 and T^2 have significant influences on migration time for BB and CCF models; all terms except T^2, V * T, C^2, and C * T have significant influences on migration time for CCC designs.

The significance of the parameters estimated by the least squares can be assessed by using classical statistical tools such as ANOVA. When different single response or multi-responses are chosen as the objective function, the most significant variables for different responses will be different. The three models were found to describe the experimental data adequately with high confidence ($p < 0.05$), and led to different coefficients of determination (R^2), the adjusted coefficients of determination ($R^2_{\text{adj.}}$), which is related to the number of parametric coefficients in the model and the predictive power of the model, which is given by the predicted R^2. In fact, the values of R^2 and $R^2_{\text{adj.}}$ are indicators of the explanatory power of the model and varies from 0, when the model does not explain the response, to 1 for a perfectly explained response. The predicted R^2 is a measure of how well the model will predict the responses for new experimental conditions. The predicted R^2 is the predictive measure corresponding to the measure of fit, while R^2 is the percent variation of the response explained by the model. It gives a lower estimate to how well the model predicts the outcome of new experiments, while R^2 gives an upper estimate. The statistical evaluation of these models is shown in Table 5. This table revealed that R^2, $R^2_{\text{adj.}}$, and the predicted R^2, were higher than 0.987, 0.970, and 0.906, respectively, indicating the good fit of these models, and allowing established response surfaces and contour plots, and predict any responses within the experimental domain.

On knowing the coefficients, the function of experimental responses related to three variables could be obtained. Based on the mathematical model, the response surface can be explored graphically. In this case, one can plot the response surfaces and their two-dimensional contour plots against two of the variables, while the third is held constant at a specified level, usually the center value. Figures 3–8 show the response surfaces and contour plots for the enantiomer separation using three designs, obtained plotting selector concentration (C) versus operation voltage (V) and selector

Table 5. Statistical evaluation of each model (date from Design-Expert, Version 7.0.1 Stat-Ease, Inc. Minneapolis, MN 55413)

		R^2	$R^2_{\text{adj.}}$	Predicted R^2
BB	R_s	0.9986	0.9969	0.9789
	T_2	0.9992	0.9981	0.9881
CCF	R_s	0.9977	0.9956	0.9627
	T_2	0.9945	0.9895	0.9389
CCC	R_s	0.9878	0.9768	0.9065
	T_2	0.9974	0.9951	0.9796

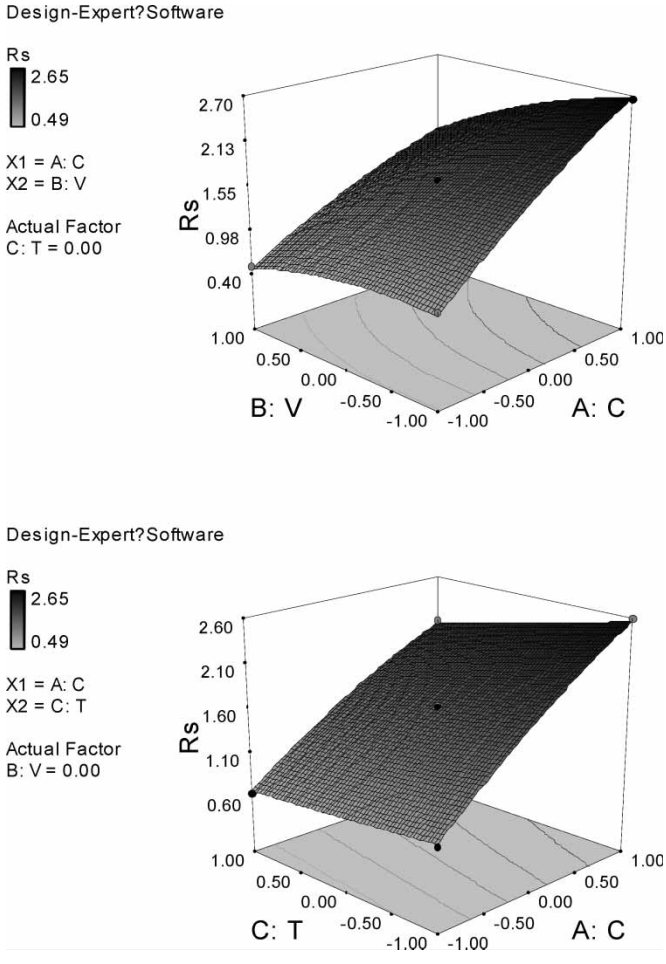

Figure 3. Response surface plot and its contour curve of R_s using BB model.

concentration versus temperature (T). It can be observed that the response (R_s) show the same behavior among three studied models. An increase in selector concentration will apparently improve the resolution, meanwhile, voltage and temperature has little effect on it. For the migration time (t_2), C has an apparent positive effect, while V has an apparent negative effect and T has also little effect on it.

Derringer's Desirability Function

Generally, responses were usually transformed into an appropriate desirability scale to balance between different responses. Frequently, different

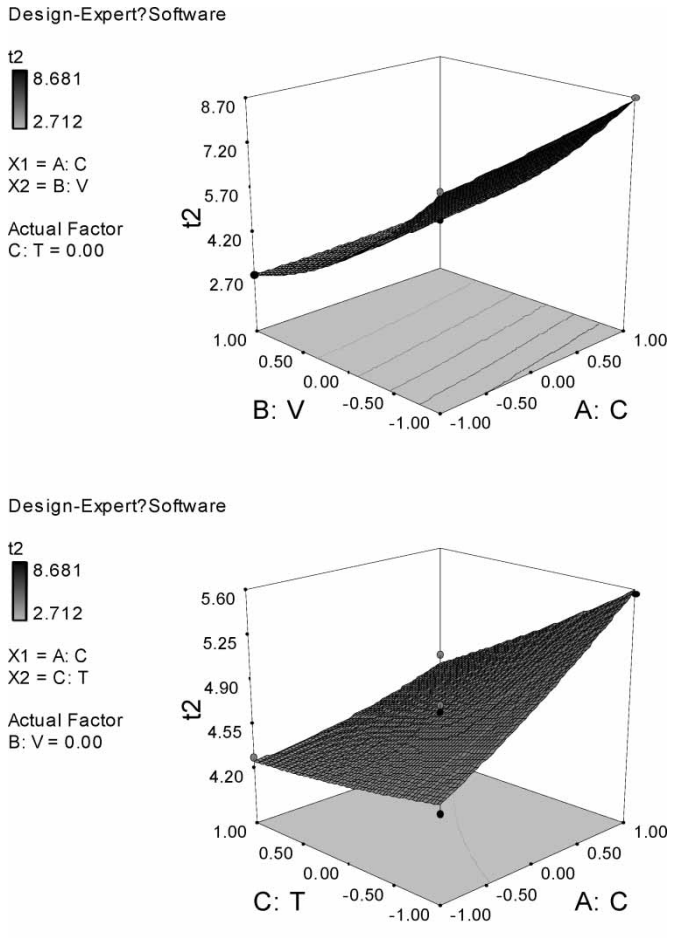

Figure 4. Response surface plot and its contour curve of t_2 using BB model.

weight factors should be assigned for each response, with larger weights corresponding to more important responses and smaller weights to less important responses.[17,29] After the individual desirabilities were calculated for each response, they were combined to provide a measure of the composite desirability of the multi-response system. This measure is the weighted geometric average of the individual desirability or the responses. Sometimes, it is very difficult to choose different weights according to the importance of different variables. The most popular methodology applied to multiple response optimization is the desirability function approach.[28,29]

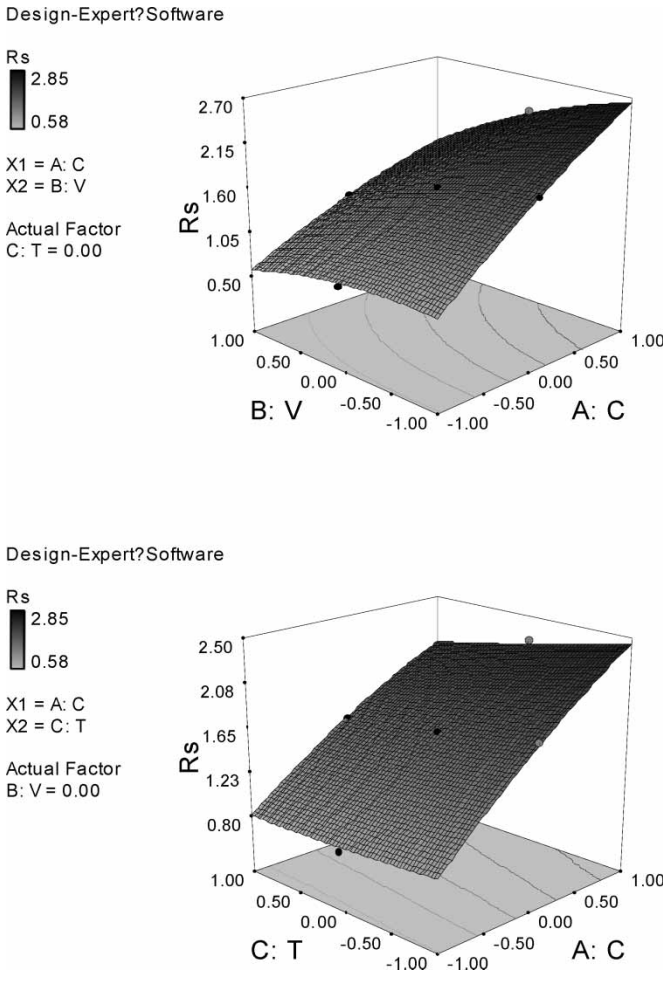

Figure 5. Response surface plot and its contour curve of R_s using CCF model.

The measured properties of each response Y_i, I = 1, 2, are transformed to a dimensionless desirability scale (d_i), defined as partial desirability function. This make it possible to combine results obtained for properties measured on different scales. The scale of the desirability function ranges between $d = 0$, for a completely undesirable response, and $d = 1$ if the response is at the target value. Once the function d_i is defined for each of the m responses of interest, an overall objective function (D), representing the global desirability function, is calculated by determining the geometric mean of the individual desirabilities. Therefore, the function D over the experimental domain is calculated as follows: $D = (\Pi\ d_i)^{1/m}$. Taking into account all requirements for m responses, we can choose the

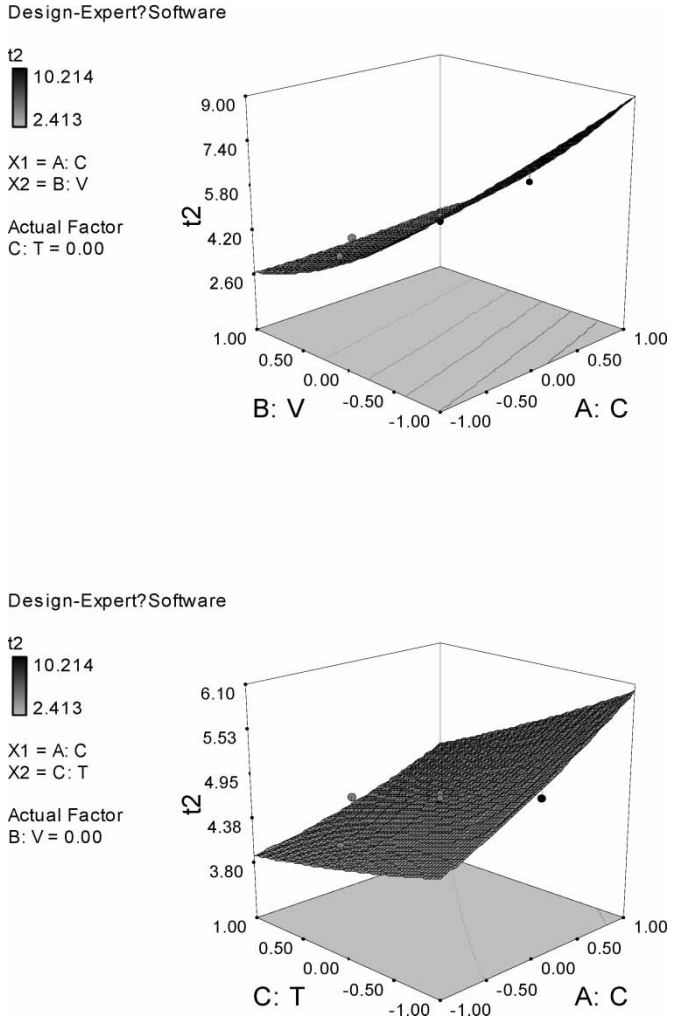

Figure 6. Response surface plot and its contour curve of t_2 using CCF model.

conditions on the design variables that maximize D. In our study, only the resolution response (R_s), and the migration time of the second enantiomer (t_2) have been considered. In order to define D quality response, t_2, and R_s were normalized. The shortest t_2 (3.0 min) and the highest R value (2.5) in all experiments were given the value 1 (maximum), while the longest t_2 (6.0 min) and the lowest R_2 values (the unwanted one, 1.0) were given the value 0 (minimum). Linear interpolation allowed us to calculate the normalized values for the remaining t_2 and R, normalized values were called d_1, and d_2, which could be calculated according to the

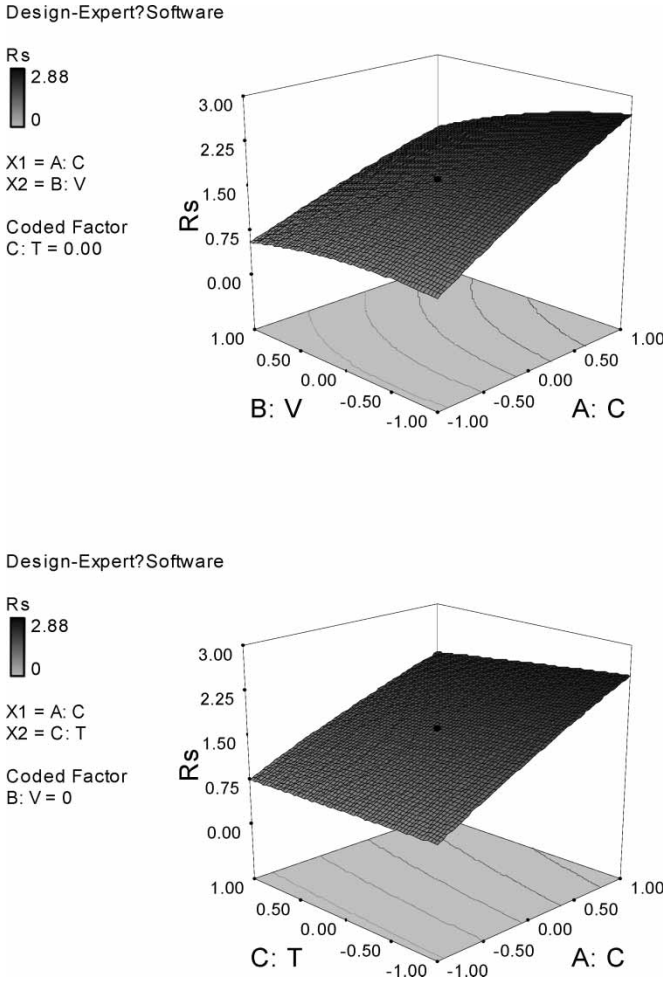

Figure 7. Response surface plot and its contour curve of R_s using CCC model.

following equations:[28,29]

$$d_1 = (R_i - R_{\min})/(R_{\max} - R_{\min}), \text{ if } 1.0 < R_i < 2.5;$$
$$d_i = 0, \text{ if } R_i \leq 1.0; d_i = 1, \text{ if } R_i \geq 2.5. \quad (1)$$

$$d_2 = (t_{\max} - t_i)/(t_{\max} - t_{\min}), \text{ if } 3.0 < t_i < 6.0;$$
$$d_i = 1, \text{ if } t_i \leq 3.0; d = 0, \text{ if } t_i \geq 6.0. \quad (2)$$

A value of D different from zero implies that all responses are in a desirable range simultaneously, and consequently, for a value of D close to 1, the combination of the different criteria is globally optimal, so as the response values are near target values (Figure 9).

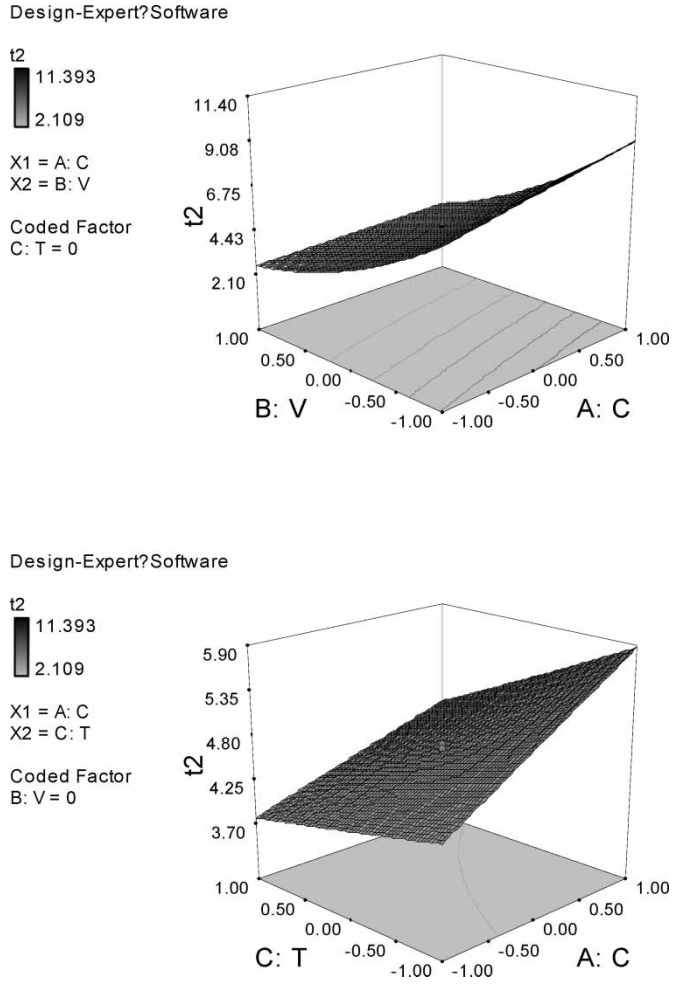

Figure 8. Response surface plot and its contour curve of t_2 using CCC model.

After calculation by the Design Expert programme, the final equations in terms of coded variables using three experimental designs were the following:

$$D_{\mathrm{BBD}} = 0.43 + 0.20X_1 + 0.16X_2 - 0.021X_3 + 0.16X_{12} + 0.041X_{13} - 0.084X_{23} - 0.096_1^2 - 0.18X_2^2 - 0.10X_3^2 \quad (3)$$

$$D_{\mathrm{CCF}} = 0.41 + 0.18X_1 + 0.16X_2 - 0.013X_3 + 0.15X_{12} - 0.017X_{13} - 0.017X_{23} - 0.11X_1^2 - 0.20X_2^2 + 0.044X_3^2 \quad (4)$$

$$D_{\mathrm{CCC}} = 0.44 + 0.15X_1 + 0.09X_2 - 0.0015X_3 + 0.15X_{12} - 0.017X_{13} - 0.017X_{23} - 0.078X_1^2 - 0.16X_2^2 - 0.026X_3^2 \quad (5)$$

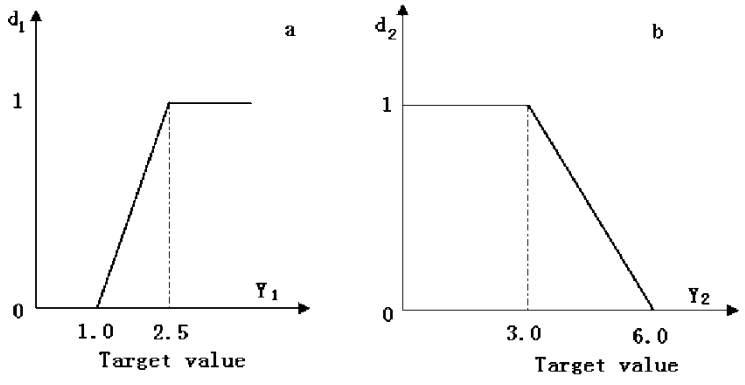

Figure 9. Shape of the d_i function associated to the response Y_i. (a) resolution (R_s); (b) migration time of the last peak (t_2).

The optimal conditions for three experimental designs were obtained with a global degree of satisfaction of *D* for the combination responses. Their coded variable values (X_1, X_2, X_3) were (1, 1, 0), (1, 1, 1), and (1, 1, 1), respectively, corresponding to their maximum D_{BBD} (0.65), D_{CCF} (0.68), and D_{CCC} (0.68), respectively. Generally, their response surfaces and contour plots of D functions could be represented and visualized for the choice of optimization conditions within the selected ranges (not shown).

The optimal electrophoretogram of three models using the desirability functions was also represented in Figure 10 a. Baseline separation of tamsulosin enantomers could be obtained during 3 min with a resolution of more than 1.5, using the optimal conditions with coded values of (1, 1, 0). Furthermore, another three experiments were performed to test the predictability of three models with a 0.10% selector, an operation voltage of 20 kV, and column temperature of 20°C, corresponding to their coded values (0, 0, 0). Their electrophoretograms have been shown in Figure 10 b, c, and d. The results from the experiments using the optimal condition and testing conditions were compared to the predicted values from three models (see Table 6). Close agreement using BB, CCF, and CCC design models could be found in most cases between observed and predicted responses.

CONCLUSIONS

The method for chiral separation of tamsulosin enantomers was optimized, which is simple, fast, and effective. The simultaneous evaluation of the experimental variables was carried out by means of BB, CCF, and CCC design models, with efficient estimation of the first and second-order coefficients. For three designs, all design points can be sure to fall within a safe operating zone, which have similar results for optimization and prediction in our

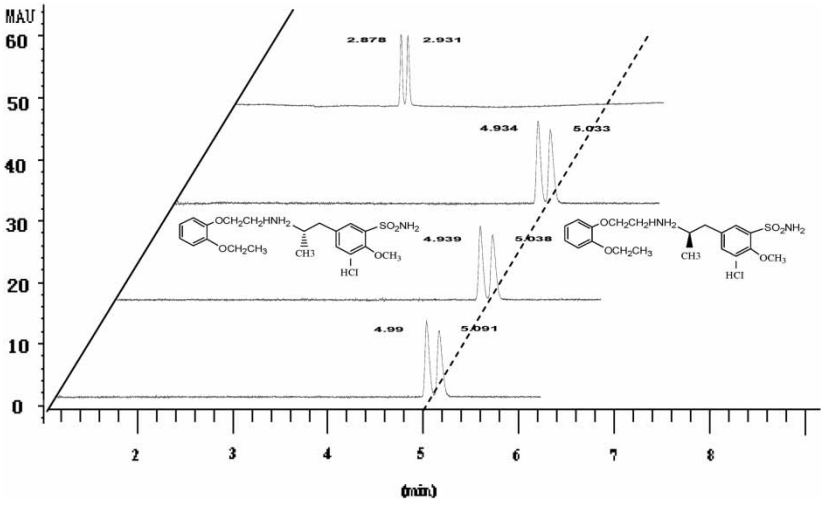

Figure 10. Electropherogram of the tamsulosin enantomers using the optimal conditions: Tris-H_3PO_4 = 100 mM, pH = 2.5, (a) 0.15% S-β-CD, 25 kV, 15°C; (b, c, d) 0.1% S-β-CD, 20 kV, 20°C. The first peak is R-TH, the second peak is S-TH.

Table 6. Observed and predicted response for testing of the predictability of the models

Response	Coded value	Experimental average value n = 3	BB Pred. value	CCF Pred. value	CCC Pred. value
R_s	(1, 1, 0)	1.62	1.66	1.59	1.68
t_2		2.93	3.00	2.88	2.82
R_s	(0, 0, 0)	1.49	1.63	1.62	1.62
t_2		5.02	4.65	4.62	4.63

studies. An appropriate use of experimental design ensures that experimental data contain maximum information and provides the availability of answers to real chemical problems, confirming how the application of chemometric techniques in analytical chemistry is needed and can be successfully realized. Compared to empirical methods, chemometrics can greatly simplify the optimization procedure finding the appropriate experimental conditions.

ACKNOWLEDGMENTS

The financial support from the NSFC-KOSEF Scientific Cooperation Program, Program for New Century Talents of University in Henan

Province, and Program for Backbone Teacher in Henan Province are acknowledged.

REFERENCES

1. Siouffi, A.M.; Phan-Tan-Luu, R. Optimization methods in chromatography and capillary electrophoresis. J. Chromatogr. A **2000**, *892*, 75–106.
2. Zhang, Y.P.; Gong, W.J.; Lee, K.P.; Choi, S.H. Computer-assisted, prediction, and multifactor optimization of hydrophobic compounds in liquid chromatography. Microchim. Acta **2005**, *152*, 113–121.
3. Jimidar, M.; Aguiar, P.F.; Pintelon, S.; Massart, D.L. Optimization and validation of an enantioselective method for a chiral drug with eight stereo-isomers in capillary electrophoresis. J. Pharm. Biomed. Anal. **1997**, *15*, 709–713.
4. Suresh Bahu, C.V.; Chung, B.C.; Yoo, Y.S. Experimetal design to investigate factors affecting capillary zone electrophoresis. Anal. Lett. **2004**, ***37***, 2485–2499.
5. Zhang, Y.P.; Lee, K.P.; Kim, S.H.; Gopalan, A.; Yuan, Z.B. Comparative study on the chiral separation of phenyl alcohols by capillary electrophoresis and liquid chromatography. Electrophoresis **2004**, *25*, 2711–2719.
6. Sentellas, S.; Saurina, J. Chemometrics in capillary electrophoresis Part A: Methods for optimization. J. Sep. Sci. **2003**, *26*, 875–885.
7. Sentellas, S.; Saurina, J. Chemometrics in capillary electrophoresis. Part B: Methods for optimization. J. Sep. Sci. **2003**, *26*, 1395–1402.
8. Gabrielsson, J.; Lindberg, N.O.; Lundstedt, T. Chemometrics in capillary electrophoresis. Part B: Methods for data analysis. J. Chemometrics **2002**, *16*, 141–160.
9. Zhang, Y.P.; Zhang, Y.J.; Gong, W.J.; Gopalan, A.I.; Lee, K.P.J. Rapid separation of Sudan dyes by reverse-phase high performance liquid chromatography through statistically designed experiments. J. Chromatogr. A **2005**, *1098*, 183–187.
10. Rudaz, S.; Cherkaoui, S.; Gauvrit, J.Y.; Lanteri, P.; Veuthey, J.L. Experimental designs to investigate capillary electrophoresis-electrospray ionization-mass spectrometry enantioseparation with the partial-filling technique. Electrophoresis **2001**, *22*, 3316–3326.
11. Ficarra, R.; Cutroneo, P.; Aturki, Z.; Tommasini, S.; Ficarra, P. An experimental design methodology applied to the enantioseparation of a non-steroidal anti-inflammatory drug candidate. J. Pharm. Biomed. Anal. **2002**, *29*, 987–997.
12. Hillaert, S.; Heyden, Y.; Bossche, W.V. Optimisation by experimental design of a capillary electrophoretic method for the separation of several inhibitors of angiotensin-converting enzyme using alkylsulphonates. J. Chromatogr. A **2002**, *978*, 231–242.
13. Smadja, C.; Potier, I.; Chaminade, P.; Jacquot, C.; Taverna, M. Comparison of On-line Preconcentration Methods for Determination of Derivatized Serotonin by CE–LIF. Chromatographia **2003**, *58*, 79–85.
14. Servais, A.C.; Fillet, M.; Chiap, P.; Abushoffa, A.M.; Hubert, P.; Crommen, J. Optimization of the separation of β-blockers by ion-pair capillary electrophoresis in non-aqueous media using univariate and multivariate approaches. J. Sep. Sci. **2002**, *25*, 1087–1095.
15. Avois, L.M.; Mangin, P.; Saugy, M. Development and validation of a capillary zone electrophoresis method for the determination of ephedrine and related compounds in urine without extraction. J. Chromatogr. B **2003**, *791*, 203–216.

16. Loukas, Y.L.; Sabbah, S.; Scriba, G.K.E. Method development and validation for the chiral separation of peptides in the presence of cyclodextrins using capillary electrophoresis and experimental design. J. Chromatogr. A **2001**, *931*, 141–152.
17. Ragonese, R.; Macka, M.; Hughes, J.; Petocz, P. The use of the Box–Behnken experimental design in the optimisation and robustness testing of a capillary electrophoresis method for the analysis of ethambutol hydrochloride in a pharmaceutical formulation. J. Pharm. Biomed. Anal. **2002**, *27*, 995–1007.
18. Hows, M.E.P.; Perrett, D.; Kay, J. Optimisation of a simultaneous separation of sulphonamides, dihydrofolate reductase inhibitors and β-lactam antibiotics by capillary electrophoresis. J. Chromatogr. A **1997**, *768*, 97–104.
19. Qi, M.L.; Wang, P.; Cong, R.H. Determination of the enantiomers of Tamsulosin hydrochloride and its synthetic intermediates by chiral liquid chromatography. Chromatographia **2004**, *59*, 251–254.
20. Matsushima, H.; Takanuki, K.I.; Kamimura, H.; Watanabe, T.; Higuchi, S. Highly sensitive method for the determination of tamusulosin hydrochloride in human plasma dialysate, plasma and urine by high performance liquid chromatography-electrospray tandem mass spectrometry. J. Chromatogr. B **1997**, *695*, 317–327.
21. Zhang, Z.F.; Yang, G.L.; Liang, G.L.; Liu, H.Y.; Chen, Y. Chiral separation of Tamsulosin isomers by HPLC using cellulose Tris (3,5-dimethylphenylcarbamate) as a chiral stationary phase. J. Pharm. Biomed. Anal. **2004**, *34*, 689–693.
22. Ding, L.; Li, L.; Tao, P.; Yang, J.; Zhang, Z.X. Quantitation of tamsulosin in human plasma by liquid chromatography-electrospray ionization mass spectrometry. J. Chromatogr. B **2002**, *767*, 75–81.
23. Kavalirova, A.; Pospisilova, M.; Karlicek, R. Enantiomeric purity determination of tamsulosin by capillary electrophoresis using cyclodextrins and a polyacrylamide-coated capillary. II Farmaco **2005**, *60*, 834–839.
24. Maier, V.; Horakova, J.; Petr, J.; Tesarova, E.; Coufal, P.; Sevcik, J. Chiral separation of tamsulosin by capillary electrophoresis. J. Pharm. Biomed. Anal. **2005**, *39*, 691–696.
25. Harang, V.; Tysk, M.; Westerlund, D.; Isaksson, D.; Johansson, G. A statistical experimental design to study factors affecting enantioseparation of propranolol by capillary electrophoresis with cellobiohydrolase (Cel7A) as chiral selector. Electrophoresis **2002**, *23*, 2306–2319.
26. Ivanovic, D.; Medenica, M.; Jancic, B.; Maenovic, A.; Markovic, S. Chemometrical approach in fosinopril-sodium and its degradation product fosinoprilat analysis. Chromatographia **2004**, *60*, S87–S92.
27. Jimidar, M.I.; Vennekens, T.; Ael, W.V.; Redlich, D.; Smet, M.D. Optimization and validation of an enantioselective method for a chiral drug with eight stereoisomers in capillary electrophoresis. Electrophoresis **2004**, *25*, 2876–2884.
28. Smet, E.; Staelens, L.; Heyden, Y.V.; Baeyens, W.R.G. Optimization of the chiral separation of some 2-arylpropionic acids on an avidin column by modeling a combined response. Chirality **2001**, *13*, 556–567.
29. Alesolo, U.; Gonzalez, L.; Jimenez, R.M.; Alonso, R.M. Multivariate optimisation of a cyclodextrin-assisted-capillary zone electrophoretic method for the separation of torasemide and its metabolites. J. Chromatogr. A **2003**, *990*, 271–279.

Received September 20, 2006
Accepted October 26, 2006
Manuscript 6944